

DEM modelling of geocells reinforced sub-ballast in rail tracks

Modélisation de la géométrie des géocellules sous-ballast renforcé dans les voies ferrées

Ngoc Trung Ngo, Buddhima Indraratna & Cholachat Rujikiatkamjorn

Centre for Geomechanics and Railway Engineering, School of Civil, Mining and Environmental Engineering, University of Wollongong, Wollongong City, NSW 2522, Australia. Email: trung@uow.edu.au

ABSTRACT: This paper presents a study of the load-deformation behaviour of geocell-reinforced subballast under cyclic loads using laboratory tests and discrete element method (DEM). A series of laboratory tests with and without geocell inclusions are carried out using a large-scale track process simulation apparatus to study the beneficial effect of the geocells in decreasing the lateral and vertical deformations of railway subballast. Numerical studies conducted in the DEM can capture the reinforcement effect of geocells, considering micromechanical analysis subjected to a given frequency and load cycles, the predicted load-settlement response of the subballast with and without geocell agrees well with those measured experimentally. This finding indicates that the proposed DEM model is able to capture the deformation behaviour of the subballast reinforced by the geocells. These observations clearly emphasise the beneficial effects of the geocell in decreasing the deformation of subballast from a micromechanical perspective.

RÉSUMÉ : Cet article présente une étude du comportement charge-déformation cyclique du sous-ballast renforcé par géocellules. Les résultats des tests en laboratoire et de la méthode des éléments discrets (DEM) est présenté. Une série d'essais en laboratoire avec et sans inclusions de géocellules est réalisée avec un appareil de simulation à grande échelle pour étudier l'effet bénéfique des géocellules, par exemple la diminution des déformations latérales et verticales du sous-ballast ferroviaire. Les études numériques menées dans le DEM peuvent capter l'effet de renforcement des géocellules, en tenant compte de l'analyse micromécanique à une fréquence et des cycles de charge. La réponse de charge-déformation prédite du sous-ballast avec et sans géocellule s'accorde bien avec celles mesurées expérimentalement. Cette constatation indique que le modèle de DEM proposé est capable de capturer le comportement de déformation du sous-ballast renforcé par les géocellules. Ces observations soulignent clairement les effets bénéfiques du géocellule dans la diminution de la déformation du sous-ballast sous une perspective micromécanique.

KEYWORDS: Railway, Subballast, Geocell, Discrete Element Modelling

1 INTRODUCTION

A railway track network holds an essential part in the transportation infrastructure worldwide. A ballasted railway track is usually used for several reasons, including economical construction cost, and ease of maintenance. Subballast commonly comprises of broadly graded, naturally occurring or processed mixtures of sand and gravel, acting as a stress reduction layer (capping layer) and preventing mutual penetration or mud-pumping (Indraratna et al. 2013; Indraratna et al. 2016; Ngo et al. 2016a). Loss of track geometry that is often associated with excessive differential settlements due to localized failure of formation (capping and subgrade), often leads to decreased stability and reduced track longevity (Indraratna et al. 2011, Rujikiatkamjorn et al. 2012). In this regard, three-dimensional cellular reinforcement, also known as geocell mattress, has been used to reduce excessive settlements and lateral displacements of ballasted rail tracks (Ngo et al. 2016b). The improved performance of geocell-stabilised granular layer has been attributed to enhanced apparent cohesion between the infilled materials and the geocell (Leshchinsky 2011). Nevertheless, recent studies have stated that the additional confinement mobilised during loadings, helps to improve confinement and minimize the deformation of infilled grains, and hence maintain stability of the infill granular material (Biabani et al. 2016a). Owing to its three-dimensional configuration, geocell arrests lateral spreading of the in-fill materials and creates a relatively stiffer mat that redistributes the applied load over a wider area. In order to study the benefit of geocells, different types of geocells have been tested. In addition, the influences of aperture size and shape and opening area have also been examined by employing large-

scale direct shear box and assessing the shear strength of unreinforced and reinforced granular materials (Biabani et al. 2016b).

There has been limited research conducted to investigate the benefit of geocells on ballasted track substructure, where the benefits of geocell under cyclic loading have not been investigated in details either in laboratory or numerical modelling (Leshchinsky et al. 2013). The development of computational models that have been fully calibrated by either laboratory or field measurements is thereby inevitable to study the improved performance of geocell-stabilised subballast and to implement systematic design guidelines for ballasted track, considering the additional confinement benefit given by geocells (Ngo et al. 2016b). This paper presents a study of using a novel Track process Simulation Apparatus (TPSA) to conduct cyclic tests of geocell-reinforced sub-ballast and to develop a discrete element model (DEM) simulating the composite system, capturing the confinement effects given by the geocell to infilled subballast grains.

The discrete element method (DEM) introduced by Cundall and Strack (1979) has been widely used to study stress-strain behaviour of granular materials (McDowell et al. 2006; Tutumluer et al. 2012; Indraratna et al. 2014; Ngo et al. 2016c). It is noted that there have been limited research on the use of DEM to simulate rail sub-ballast under cyclic loads with high numbers of load cycles. Ngo et al. (2014) conducted DEM analysis to investigate the performance of geogrid stabilised ballast fouled with coal, and presented that the interlock of the aggregates with geogrid was the main causes for improved performance of the composite assembly. It would also be noted that there has been limited past DEM studies on the behavior of geocell-reinforced ballast under a high numbers of load cycles and varied frequencies.

In this study, laboratory tests are carried out and the discrete element method (DEM) is employed to model geocell-reinforced sub-ballast subjected to cyclic train loading, capturing the deformation and corresponding stress distributions of this composite assembly.

2 LABORATORY STUDY

A large-scale Track Process simulation Apparatus (TPSA: 800 mm long, 600 mm wide and 600 mm high) was designed and built at the University of Wollongong (Figure 1), and it was used in this study to examine the load-deformation responses of the unreinforced and geocell-reinforced subballast subjected to cyclic loading. Subballast material had a total depth of 450 mm, of which the upper 150mm was reinforced by geocells, as illustrated in Figure 1. Subballast used in the laboratory was a locally available crushed basalt, collected from a quarry near Wollongong (NSW, Australia). The particle size distribution used for the sub-ballast followed the Australian rail industry specified range ($D_{50} = 3.3$ mm, $D_{max} = 19$ mm, $D_{min} = 0.075$ mm, $C_u = 16.3$, $C_c = 1.3$, unit weight, $\gamma = 18.5$ kN/m³). Geocells made from polyethylene, that was connected at the joints to form a three-dimensional cellular configuration (i.e. having depth = 150 mm, ultimate tensile strength = 9.5 kN/m, thickness = 1.3 mm, density = 950 kg/m³) was used. A predetermined weight of subballast was placed inside the TPSA box in several layers and compacted using a vibratory hammer to achieve a relative density of around 77%, which is representative of the density of subballast in the field (Biabani et al. 2016b). A geocell mattress was then placed onto the surface of the compacted subballast followed by the placement of subballast layer on the top of the geocell. All specimens were prepared until the layer of sub-ballast reached a final height of 450 mm.

The experiments were conducted under plane strain condition, where any lateral movement in the longitudinal direction (parallel to the track) was restricted ($\epsilon_2=0$). The walls were allowed to move laterally in the direction parallel to the sleeper (or tie) ($\epsilon_3 \neq 0$), to model a long straight section of track. Laboratory tests were carried out in a stress-controlled manner, where the magnitudes of the cyclic stresses were calculated based on 30 tons/axle load subject to different confining pressures of, $\sigma_3 = 5, 10, 15, 20, 30$ kPa and frequencies of $f=10, 20, 30$ Hz. Initially, a monotonic strain-controlled load was applied to the specimen at a rate of 1 mm/min until a mean level of cyclic deviator stress was achieved. Subsequently, a stress controlled cyclic loading using a positive full-sine waveform was applied to the specimens where a maximum and minimum stress of $q_{max} = 166$ kPa and $q_{min} = 41$ kPa was used to simulate subballast under a heavy haul freight network operating in NSW (Ngo and Indraratna 2016).

3 DISCRETE ELEMENT MODELLING OF TPSA

Discrete Element Method (DEM) was used to model the interaction between geocell and subballast by modelling the Track Process Simulation Apparatus (TPSA), as illustrated in Figure 2. The angular-shaped grains of sub-ballast were simulated by connecting a number of circular-shaped particles together, mimicking the actual sub-ballast shape and angularity. A total of 26567 particles, with sizes ranging from 0.5 to 19 mm, were generated to simulate actual sub-ballast gradation with a representative field unit weight approximately of 18.5 kN/m³. Particles were placed in the assembly at random orientations to mimic laboratory conditions. The geocell pocket

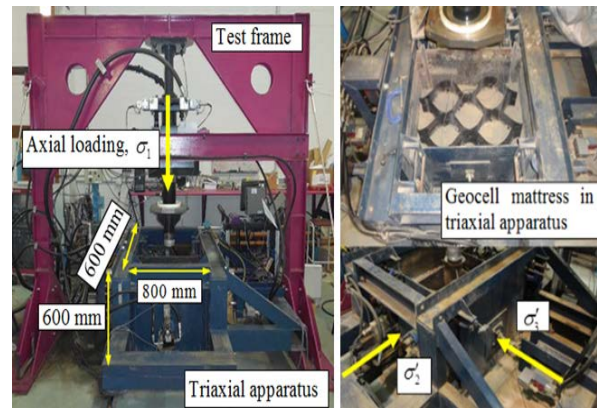


Figure 1. Track Process Simulation Apparatus (TPSA)

structure was modeled by bonding balls of 20 mm-diameter and 10 mm-diameter to form vertical and horizontal panels, respectively. This simplified geocell structure was presumed to be adequate to provide the confinement effect for the subballast packed inside the cellular pockets. Micromechanical parameters to model subballast and geocells (e.g. shear and normal contact stiffness, friction coefficient) adopted in the current DEM analysis were determined based on calibration of DEM analysis with the laboratory data, as given in Table 1.

Table 1. Micromechanical parameters used to model subballast and geocell in DEM.

Parameters	Sub-ballast	Geocell
Particle density (kN/m ³)	15.5	18.5
Coefficient of friction	0.72	0.45
Contact normal stiffness (N/m)	2.56 E8	6.51 E6
Contact shear stiffness, k_s (N/m)	2.56 E8	6.51 E6
Contact bond normal strength, ϕ_n (kN)	5.36 E6	43.2
Contact bond shear strength, ϕ_s (kN)	8.53 E6	43.2
Parallel bond radius multiplier, r_p	0.5	0.5
Parallel bond normal stiffness, k_{np} (kPa/m)	4.86 E7	4.86 $\times 10^7$
Parallel bond shear stiffness, k_{sp} (kPa/m)	4.86 E7	4.86 $\times 10^7$
Parallel bond normal strength, σ_{np} (MPa)	352	352
Parallel bond shear strength, σ_{sp} (MPa)	352	352

4 RESULTS AND DISCUSSION

4.1 Vertical deformation with and without Geocell

Settlements of subballast at varying load cycles predicted from DEM simulations compared to the those measured experimentally are presented in Figure 3. Results obtained from DEM analysis matched reasonably well with the experimental data at any given frequency and confining pressure. The predicted and measured data showed that the settlement increased with an increase in frequency. Geocell-reinforced subballast experienced less settlement than that of the unreinforced assembly. Undoubtedly, this is a result of additional confinement given by the geocell that would decrease the deformation of sub-ballast. When the subballast grains were compacted over a geocell, they were projected through the geocell pockets and generated a strong mechanical interlock (i.e. non-displacement boundary conditions) which results in decreased deformation. Moreover, the settlement increased significantly during the first few thousand cycles due to initial particle compression and rearrangement, and then the settlement increased at a diminished rate in the subsequent load cycles and approached an approximately constant after around 8000 load cycles.

4.2 Contact force distributions

Contact forces in a subballast specimen are transferred through an inter-connected network of force chains. Figure 4a shows contact force distributions of an unreinforced subballast specimen subjected to the cyclic load at a given frequency of 20 Hz at a settlement of 5 mm, while Figures 4b-d present the contact force distributions of geocell-reinforced subballast at settlements of S=5 mm, 15 mm, and 20 mm, respectively. The contact forces are plotted as lines on the same scale, whose thickness is proportional to its magnitude, and for clarity, only those contacts with a magnitude exceeding average forces of the whole assembly are showed. It is seen that the total number of contact forces and maximum contact forces increase as settlement increases, and this can be attributed to the assembly was compacted and compressed to support the applied loads. For instance, with reinforced sub-ballast, the number of contacts is 60,252 for the settlement of 5 mm, and it increases to 78,252 and 83,521 contacts for settlements of S=15 and 20 mm, respectively. Maximum contact forces also increases with an increase of settlements, and these are 745 N, 857 N and 946 N for the settlements of S=5, 15 and 20 mm, respectively. Compared to the unreinforced subballast assembly (Figure 4a), the reinforced assemblies created more contacts within the geocell regions, and this could be due to the confinement the geocell given to the infilled aggregates. It can also be seen that the tensile forces (in red colour) in geocells are mobilised with an increased in settlement.

4.3 Distributions of contact normal and shear forces

Figure 5 shows the variations of contact normal and shear forces with depth for reinforced and unreinforced subballast (at N=10,000 cycles). Compared to the unreinforced cases (Figures 5c, 5d), geocell-reinforced subballast specimens show a significant increase in the contact force within the geocell zone, but underneath the geocell the average normal and shear contact forces decrease with depth and approach almost constant values close to the bottom of the sample. It is noted that the DEM analysis for the geocell-reinforced subballast conducted in this study was limited to the distribution of contact force chains and the average contact normal and shear force distributions. However, the comparison of the experimental observations with the 2D plane strain DEM analysis proves that to the current analysis was able to capture the load-deformation behaviour of geocell-stabilised subballast in spite of these limitations. Generally, the authors have made a few simplifications to keep the DEM analysis fairly simples, as the geocell decreases the shear and normal contact force in subballast below the geocell. It is worth mentioning that due to the brevity of this paper would not allow the reporting of more detailed DEM analyses that could capture other micro-mechanical aspects such as the evolution of fabric anisotropy and complex detailing of changing angularity with the high number of loading cycles (Ngo et al. 2016d).

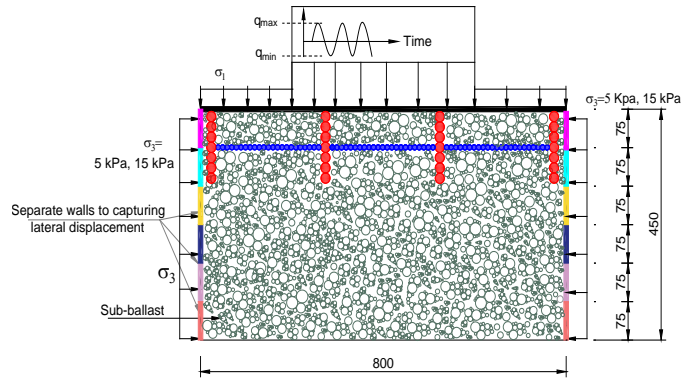


Figure 2. DEM model for subballast-geocell interactions

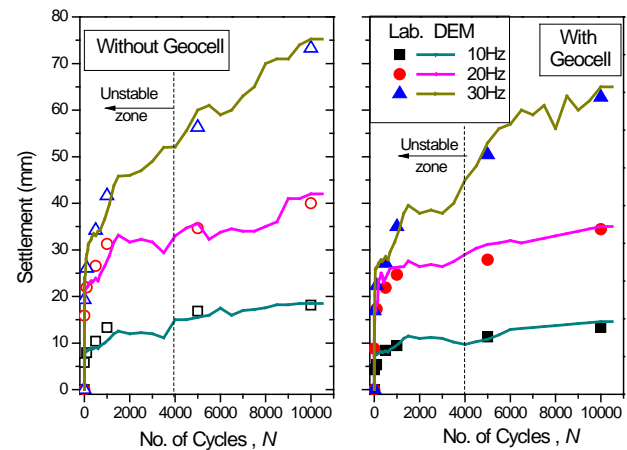
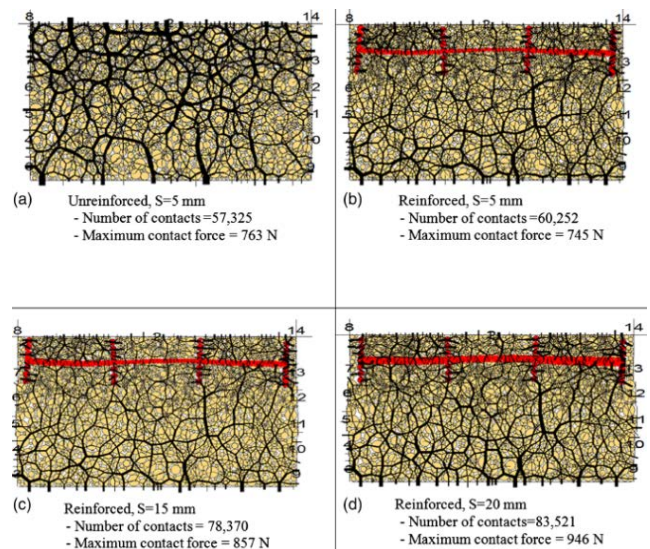


Figure 3. Settlement responses observed in laboratory and predicted in



DEM (modified after Ngo et al. 2015)

Figure 4. Distribution of contact forces for unreinforced and reinforced subballast at varied settlements (modified after Ngo et al. 2015)

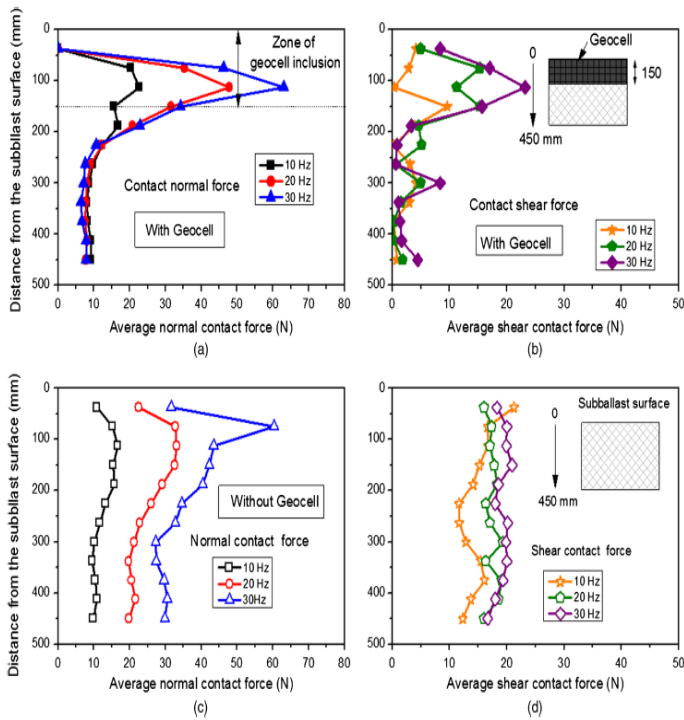


Figure 5. Distributions of contact normal and shear forces: (a) and (b) - with geocell inclusion; (c) and (d) - without geocell.

5 CONCLUSIONS

A series of large-scale laboratory tests using Track Process Simulation Apparatus were carried out on sub-ballast with and without geocell inclusion, and then the results were used to validate and compare with the DEM simulations. Irregular particles of subballast were modeled by connecting circular balls together to mimic appropriate angularity. Geocell was modelled by bonding small balls together to form the cellular pockets using contact and parallel bonds. Experimental data of settlements and lateral displacements were comparable with those obtained from DEM simulations at a given frequency and confining pressure, indicating that the DEM model proposed in this study could simulate the load-deformation responses of geocell-stabilised subballast specimens. As the frequency increased, the settlement and lateral deformations of subballast increased, but unlike the unreinforced specimen, the geocell-reinforced subballast showed significantly less settlement. This was undoubtedly due to the confinement provided by geocell that prevented sub-ballast aggregates from free movement that would otherwise occur.

Contact force distributions of geocell-reinforced sub-ballast were presented. DEM results showed that the total number of contact force distributions and the maximum contact force increased with increased deformation. The contact normal and shear forces developed among sub-ballast particles at varied depths were also captured. The magnitudes of these forces within the geocell zone were considerably higher than at other locations. Underneath the geocell, these contact forces continuously decreased with depth and approached almost constant values near the bottom of the granular assembly.

6 ACKNOWLEDGEMENTS

The Authors would like to acknowledge the CRC-Rail Manufacturing for providing the financial support (Project R2.5.1). The Authors are grateful to Mr. Alan Grant, Mr. Cameron Neilson, and Mr. Ritchie McLean for their assistance

in the laboratory. Laboratory work conducted by Dr. Biabani is also greatly appreciated. The Authors would also appreciate the kind permission from the Journal of Geotechnical and Geoenvironmental Engineering - ASCE for reproducing selected content in this paper

4 REFERENCES

- Biabani, M., Ngo, N.T., Indraratna. (2016a). "Performance evaluation of railway subballast stabilised with geocell based on pull-out testing." *Geotextiles and Geomembranes*, 44(4), pp: 579-591.
- Biabani, M.M., Indraratna, B. and Ngo, N.T. (2016b). Modelling of geocell-reinforced subballast subjected to cyclic loading. *Geotextiles and Geomembranes*, 44(4), pp: 489-503.
- Cundall, P.A., Strack, O.D.L.(1979). A discrete numerical model for granular assemblies. *Géotechnique*. 29(1), 47-65.
- Indraratna, B., Ngo, N.T. and Rujikiatkamjorn, C. (2011). Behavior of geogrid-reinforced ballast under various levels of fouling. *Geotextiles and Geomembranes*, 29(3), pp: 313-322.
- Indraratna, B., Ngo, N.T. and Rujikiatkamjorn, C. (2013). Deformation of coal fouled ballast stabilized with geogrid under cyclic load. *Journal of Geotechnical and Geoenvironmental Engineering*, 139(8), pp: 1275-1289.
- Indraratna, B., Ngo, N.T, Rujikiatkamjorn, C., and Vinod, J. (2014). Behavior of Fresh and Fouled Railway Ballast Subjected to Direct Shear Testing: Discrete Element Simulation. *International Journal of Geomechanics*. 14(1): 34-44.
- Indraratna, B., Nimbalkar, S.S., Ngo, N.T. and Neville, T. (2016). Performance improvement of rail track substructure using artificial inclusions – Experimental and numerical studies." *Transportation Geotechnics*, 8, pp: 69-85.
- Leshchinsky, B. (2011). "Enhancing Ballast Performance Using Geocell Confinement". Proceedings of Geo-Frontiers. 4693-4072.
- Leshchinsky, B. and Ling, H. (2013). Effects of geocell confinement on strength and deformation behavior of gravel. *Journal of Geotechnical and Geoenvironmental Engineering*.139(2), 340-352.
- McDowell, G. R., Harireche, O., Konietzky, H., Brown, S. F. , and Thom, N. H. (2006). "Discrete element modelling of geogrid-reinforced aggregates". *Proceedings of the ICE - Geotechnical Engineering* 159(1): 35-48.
- Ngo, N.T., Indraratna, B., Rujikiatkamjorn, C. and Biabani, M.M. (2016a). Experimental and Discrete Element Modeling of Geocell-Stabilized Subballast Subjected to Cyclic Loading. *Journal of Geotechnical and Geoenvironmental Engineering*, 142(4), pp: 04015100.
- Ngo, N.T., Indraratna, B. and Rujikiatkamjorn, C. (2016b). Modelling geogrid-reinforced railway ballast using the discrete element method. *Transportation Geotechnics*, 8(2016), pp: 86-102.
- Ngo, N., Indraratna, B., and Rujikiatkamjorn, C. (2016c). "Simulation Ballasted Track Behavior: Numerical Treatment and Field Application." *Int. J. Geomech.* 10.1061/(ASCE)GM.1943-5622.0000831 , 04016130..
- Ngo, N.T, Indraratna, B., and Rujikiatkamjorn, C. (2016d). "Micromechanics-Based Investigation of Fouled Ballast Using Large-Scale Triaxial Tests and Discrete Element Modeling." *Journal of Geotechnical and Geoenvironmental Engineering* 10.1061/(ASCE)GT.1943-5606.0001587 , 04016089.
- Ngo, N.T. and Indraratna, B.: Improved performance of rail track substructure using synthetic inclusions: Experimental and numerical investigations." *Int J Geosynth and Ground Eng*, 2(3), 1-16 (2016)
- Ngo, N. T., Indraratna, B. , and Rujikiatkamjorn, C. (2014). "DEM simulation of the behaviour of geogrid stabilised ballast fouled with coal". *Computers and Geotechnics*. 55: 224-231.
- Rujikiatkamjorn, C., Indraratna, B., Ngo, N.T., Coop, M. (2012) A laboratory study of railway ballast behaviour under various fouling degree. In: *Proceedings of the 5th Asian Regional Conference on Geosynthetics*.
- Tutumluer, E., Huang, H., and Bian, X. (2012). "Geogrid-aggregate interlock mechanism investigated through aggregate imaging-based discrete element modeling approach." *International Journal of Geomechanics*, ASCE. 12(4): 391-398.